Membrane Stiffness and Channel Function†

J. A. Lundbæk,*,‡,§ P. Birn,§ J. Girshman,‡ A. J. Hansen,§ and O. S. Andersen*,‡

Department of Physiology and Biophysics, Cornell University Medical College, New York, New York 10021, and Department of Neuropharmacology, Novo-Nordisk A/S, Novo-Nordisk Park, DK 2760 Måløv, Denmark

Received September 19, 1995; Revised Manuscript Received January 16, 1996⊗

ABSTRACT: Alterations in the stiffness of lipid bilayers are likely to constitute a general mechanism for modulation of membrane protein function. Gramicidin channels can be used as molecular force transducers to measure such changes in bilayer stiffness. As an application, we show that N-type calcium channel inactivation is shifted reversibly toward negative potentials by synthetic detergents that decrease bilayer stiffness. Cholesterol, which increases bilayer stiffness, shifts channel inactivation toward positive potentials. The voltage activation of the calcium channels is unaffected by the changes in stiffness. Changes in bilayer stiffness can be predicted from the molecular shapes of membrane-active compounds, which suggests a basis for the pharmacological effects of such compounds.

Changes in membrane lipid composition alter the bilayer mechanical properties (Evans & Needham, 1987) and the function of integral membrane proteins. Specifically, the function of integral membrane proteins varies with lipid bilayer thickness (Caffrey & Feigenson, 1981; Johannsson et al., 1981; Criado et al., 1984; Baldwin & Hubbell, 1985b; Brown, 1994) and monolayer equilibrium curvature (Navarro et al., 1984; Jensen & Schutzbach, 1984; Hui & Sen, 1989; Brown, 1994; McCallum & Epand, 1995). Such control of protein function can arise from hydrophobic coupling between bilayer and imbedded proteins, because conformational changes in the proteins' membrane-spanning domains (Unwin & Ennis, 1984; Unwin et al., 1988; Salamon et al., 1994) will deform the surrounding bilayer (Mouritsen & Bloom, 1984; Gruner, 1991; Andersen et al., 1992; Brown, 1994; Lundbæk & Andersen, 1994). Changes in the bilayer deformation energy (ΔG^0_{def})[1] alter the free energy difference between different protein conformations (Figure 1*a*), which in turn will alter function.

To a first approximation (Mouritsen & Bloom, 1984; Huang, 1986; Durkin et al., 1993), ΔG^0_{def} can be expressed using a linear spring model, in which case ΔG^0_{def} will be a quadratic function of the membrane deformation (μ), the sum of the deformation depths of the two monolayers (u_1 and u_2, Figure 1*a*):

$$\Delta G^0_{def} = A\mu^2 \qquad (1)$$

where A is a bilayer stiffness coefficient whose magnitude is determined by the bilayer compressibility and bending moduli as well as the spontaneous monolayer curvature (Huang, 1986; Gruner, 1989; Hui & Sen, 1989; Dan et al.,

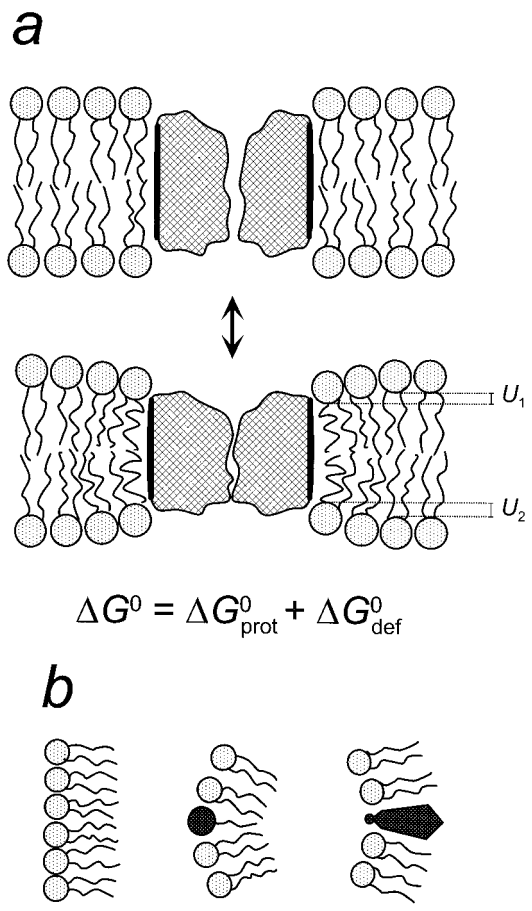

FIGURE 1: (*a*) Protein conformational changes involving the hydrophobic exterior of a membrane protein will alter the structure of the surrounding bilayer. The bilayer deformation can be described by the linear extent of the deformation in the two monolayers (u_1 and u_2). The free energy difference (ΔG^0), between the conformational states of the protein, is the sum of the intrinsic free energy change in the protein (ΔG^0_{prot}) and the bilayer deformation energy (ΔG^0_{def}). (*b*) Bilayer-forming lipids have a cylindrical shape (left), cone-shaped molecules promote micelles with a convex surface (middle), and cholesterol has an inverted cone shape and can promote H_{II} phase structures with a concave surface (right).

†Supported in part by NIH Grant GM21342 (O.S.A.) and by a grant from the Danish Medical Research Council (J.A.L.).

* To whom correspondence should be sent.

‡ Cornell University Medical College.

§ Novo-Nordisk A/S.

⊗ Abstract published in *Advance ACS Abstracts,* March 1, 1996.

[1] Abbreviations: ΔG^0_{def}, bilayer deformation energy; u, depth of bilayer deformation; A, bilayer stiffness coefficient; TX100, Triton X-100; βOG, β-octyl glucoside; gA, gramicidin A; IMR32 cells, a human neuroblastoma cell line; DOPC, dioleoylphosphatidylcholine; τ, average duration of gA channels; TTX, tetrodotoxin; CMC, critical micellar concentration; sd, standard deviation; sem, standard error of the mean; n, number of independent observations.

0006-2960/96/0435-3825$12.00/0 © 1996 American Chemical Society

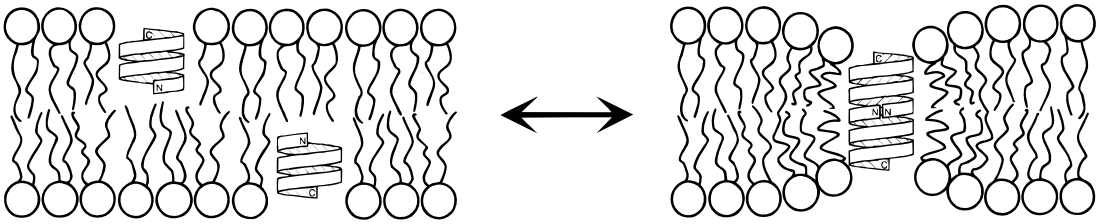

FIGURE 2: Gramicidin channel formation involves a convex deformation of the monolayers [after Andersen et al. (1995)].

1994). The quantitative relationship between changes in these parameters and the magnitude of A is complex, however, as changes in either modulus as well as the spontaneous monolayer curvature affect the magnitude of both the bending and the compression components of ΔG^0_{def} (C. Nielsen, M. Goulian, and O. S. Andersen, unpublished results). Given this complexity, it is helpful to take a heuristic approach.

The spontaneous monolayer curvature is determined by the average shape of the molecules in the monolayer (Figure 1*b*) (Cullis & deKruijff, 1979; Mitchell & Ninham, 1981). Molecules with a cylindrical shape form planar monolayers (no curvature, Figure 1*b*, left). Molecules with a cone shape, such as Triton X-100 (TX100) and β-octyl glucoside (βOG), are micelle-forming and promote convex monolayer curvatures (Figure 1*b*, middle). Molecules with an inverted cone shape, such as cholesterol, promote H_{II} phases (Seddon, 1990) and concave monolayer curvatures (Figure 1*b*, right). TX100 and βOG, on the one hand, and cholesterol, on the other, therefore would be expected to have opposite effects on bilayer stiffness.

In order to examine the relation between molecular shape, bilayer stiffness, and the function of integral membrane proteins, we investigated the effects of TX100, βOG, and cholesterol on the function of N-type voltage-dependent calcium channels. The function of voltage-dependent calcium channels is modified by a variety of amphipathic compounds [e.g. Janis et al. (1987) and Hille (1992)]. The pharmacological specificity is often modest, and alterations in channel function could reflect altered bilayer−protein interactions due to altered bilayer stiffness. We tested this hypothesis by measuring the effect of TX100, βOG, and cholesterol on the stiffness of dioleoylphosphatidylcholine (DOPC)/*n*-decane bilayers *in vitro* and on the function of N-type calcium channels in IMR32 cells.

The effects on bilayer stiffness were measured using gA channels as molecular force transducers. gA channels can be used to estimate changes in stiffness because they are dimers, formed by the transmembrane association of a monomer from each monolayer [O'Connell et al., 1990; see Andersen and Koeppe (1992) for a review of gramicidin channel structure and function]. This monomer−dimer transition constitutes a well-defined "conformational" change (Figure 2). The length of the channel's hydrophobic exterior (~2.17 nm; Elliott et al., 1983) is less than the hydrophobic thickness of a DOPC/*n*-decane bilayer (~5 nm; Benz & Janko, 1976; see also Table 1). gA channel formation therefore produces a defined bilayer deformation with a convex monolayer curvature. Alterations in the average channel duration (τ) directly reflect changes in the bilayer stiffness (for this bilayer deformation).

MATERIALS AND METHODS

Planar Lipid Bilayer Experiments. Single channel currents were measured in unbuffered 1.0 M NaCl (25 ± 1 °C) using the bilayer punch (Andersen, 1983). gA was a gift from R. E. Koeppe II (University of Arkansas). βOG and TX100 were added to the electrolyte solution, and cholesterol was present in the bilayer-forming solution (DOPC:cholesterol = 1:2). Membrane potential = 200 mV; the current signal was filtered at 50−100 Hz, digitized at 6 times the filter frequency, and sampled by computer (Andersen, 1983; Sawyer et al., 1989). For each experimental condition, τ was estimated by fitting single exponential distributions, $N(t)/N(0) = \exp(-t/\tau)$, where $N(t)$ is the number of channels with a duration longer than time t, to the duration distributions.

The specific membrane capacitance (C_m) was measured using a sawtooth potential across planar bilayers with an area of ~1.5 mm^2. The bilayer area was measured using a microscope with a calibrated reticule. The membrane thickness, d, was calculated from C_m:

$$d = \epsilon_o \epsilon_r / C_m \qquad (2)$$

where ϵ_o denotes the permittivity of free space and ϵ_r is the relative dielectric constant, which is assumed to be 2.1 (similar to the value for bulk hydrocarbons).

Cell Culture and Whole-Cell Voltage-Clamp Experiments. IMR32 cells (American Type Culture Collection) were grown on cover slips in MEM with Earle's salt (Gibco) containing 10% heat-inactivated fetal bovine serum and 50 μg/mL gentamicin (37 °C, ambient atmosphere with 5% CO_2). Differentiation was initiated by 2.5 μM 5-bromo-2′-deoxyuridine.

The cholesterol content of cell membranes was enriched using a modified version of the method of Bolotina et al. (1989). Cholesterol (20 mg) dissolved in 1 mL of tetrahydrofuran was added to 100 mL of a vigorously stirred, phosphate buffered, saline solution (Dulbecco) containing 10% heat-inactivated fetal bovine serum. A control medium was prepared by dissolving 1 mL of tetrahydrofuran (in the absence of cholesterol) in a similar solution. Cholesterol-enriched and control media were lyophilized and stored at 5 °C. Prior to use, these media were redissolved in water to a final cholesterol concentration of 0.5 mM (in the cholesterol-containing solution). The cells were incubated for 20−24 h before use.

Patch-clamp studies were conducted 10−21 days after differentiation. The channels were primarily N-type calcium channels (Carbone et al., 1990), as confirmed by the finding that 5 μM ω-conotoxin (MVIIA) inhibited 85−95% of the current elicited at a test potential of +10 mV from a holding potential of −80 mV (results not shown). The (extracellular) bath solution was 80 mM TEACl, 30 mM $BaCl_2$, 1 mM $MgCl_2$, 10 mM HEPES, 10 mM glucose, and 0.2 μM TTX

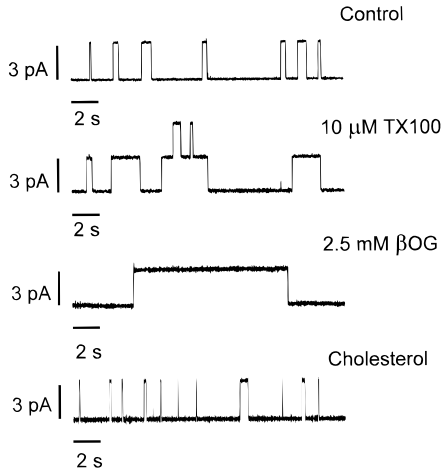

FIGURE 3: Single channel current traces, to show the effect of βOG, TX100, and cholesterol on gA channels in DOPC/*n*-decane bilayers. The average single channel durations are summarized in Table 1.

(pH 7.3). The (intracellular) electrode solution was 100 mM CsCl, 40 mM HEPES, 2.5 mM $MgCl_2$, 10 mM EGTA, 2.9 mM $CaCl_2$, 1 mM Na_2ATP, and 0.3 mM Na_3GTP (pH 7.2). The temperature was 22−25 °C. The extracellular solutions were changed using a fast superfusion system (Konnerth et al., 1987). Measurements were done using 1−3 MΩ electrodes. Voltage pulse generation and data acquisition were controlled using pClamp (Axon Instruments, Foster City, CA). Pipette and membrane capacitances were compensated for electronically. The series resistance errors were <5 mV. The current signal usually was filtered at 1 kHz and digitized at 2 kHz. Leak current corrections were done using a −120 mV pulse following all test pulses. The leak current−voltage relations were determined in the presence of 100 μM Cd^{2+}. The leak current varies as a nonlinear function of membrane potential, but the nonlinearity was not affected by the presence of 2.5 mM βOG, 10 μM TX100, or cholesterol enrichment (results not shown). The leak currents at +10 mV, the test potential used to measure the steady-state inactivation curves, therefore were estimated using the ratio of the measured leak currents at +10 and at −120 mV (measured in the presence of 100 μM Cd^{2+}).

RESULTS AND DISCUSSION

Bilayer Experiments. gA channels were used to measure the effects of TX100, βOG, and cholesterol on the stiffness of dioleoylphosphatidylcholine (DOPC)/*n*-decane bilayers. Figure 3 shows the effects of TX100, βOG, and cholesterol on gA channels in DOPC bilayers. βOG and TX100 increased τ; cholesterol decreases τ. These results are in accord with earlier findings that micelle-forming compounds decrease bilayer stiffness (Sawyer et al., 1989; Andersen et al., 1992, 1995; Lundbæk & Andersen, 1994), whereas H_{II}-phase-promoting compounds increase the stiffness (Pope et al., 1982; Andersen et al., 1995).

βOG and TX100 had no effect on the specific capacitance of DOPC/*n*-decane bilayers (Table 1); that is, these compounds do not affect membrane thickness (cf. eq 2). Addition of cholesterol to the membrane-forming solution increased the specific capacitance, indicating that the membrane thickness was decreased (Table 1). The cholesterol-induced changes in membrane capacitance agree with those described earlier (Hanai et al., 1965a).

To relate changes in τ_c to changes in membrane stiffness, as summarized by *A*, we note that the overall free energy for channel formation (ΔG^0) is the sum of contributions due to the channel molecule itself (ΔG^0_{prot}) and to the membrane deformation (ΔG^0_{def}, eq 1):

$$\Delta G^0 = \Delta G^0_{prot} + \Delta G^0_{def} = \Delta G^0_{prot} + \alpha\mu^2 \qquad (3)$$

The transition state for channel dissociation occurs when the two monomers move a distance δ apart. The activation energy for channel dissociation ($\Delta G^{\ddagger}$) is comprised of two terms: the intrinsic activation energy ($\Delta G^{\ddagger}_{prot}$) and the difference in bilayer deformation energy for a deformation of μ and of $\mu - \delta$,

$$\Delta G^{\ddagger} = \Delta G^{\ddagger}_{prot} + \Delta G^{\ddagger}_{def} \qquad (4)$$

or, using eq 3,

$$\Delta G^{\ddagger} = \Delta G^{\ddagger}_{prot} + A[(\mu - \delta)^2 - \mu^2] = \Delta G^{\ddagger}_{prot} - A(2\mu - \delta)\delta \qquad (5)$$

The average duration of gA channels varies with the general phase preference and molecular shape of the membrane-forming molecules with no evidence for chemical specificity (Neher & Eibl, 1977; Sawyer et al., 1989; Lundbæk & Andersen, 1994; Maer et al., 1995); specific interactions between gA and membrane-forming, or membrane-modifying, molecules have not been described. Changes in τ, i.e. in $\Delta G^{\ddagger}$, therefore most likely reflect changes in $\Delta G^{\ddagger}_{def}$ only:

$$\Delta\Delta G^{\ddagger} = \Delta\Delta G^{\ddagger}_{def} = \Delta G^{\ddagger,mod}_{def} - \Delta G^{\ddagger,cntr}_{def} = RT \ln(\tau^{mod}/\tau^{cntr}) \qquad (6)$$

where the superscripts cntr and mod denote control and modifier, respectively, *R* is the gas constant, and *T* is the temperature in Kelvin (the membrane deformation energy will tend to pull the dimer apart; a decrease in ΔG^0_{def} will *increase* $\Delta G^{\ddagger}_{def}$ and τ).

Changes in $\Delta G^{\ddagger}_{def}$ result from changes in *A*, μ, or both. Using eqs 5 and 6

$$\Delta\Delta G^{\ddagger} = A^{cntr}(2\mu^{cntr} - \delta)\delta - A^{mod}(2\mu^{mod} - \delta)\delta \qquad (7)$$

and

$$A^{mod} = \frac{A^{cntr}(2\mu^{cntr} - \delta) - \Delta\Delta G^{\ddagger}/\delta}{2\mu^{mod} - \delta} = A^{cntr}\frac{2\mu^{cntr} - \delta}{2\mu^{mod} - \delta} + \frac{RT \ln(\tau^{cntr}/\tau^{mod})}{(2\mu^{mod} - \delta)\delta} \qquad (8)$$

A^{cntr} for phospholipid bilayers has been estimated previously to be ~120 kJ/(mol·nm^2) (Durkin et al., 1993) or ~50*RT* (a similar estimate has been deduced from changes in τ as a

[2] This separation corresponds to the two monomers being moved apart (rotated) to the point where the dimer is stabilized by four rather than six hydrogen bonds (as is normally the case). Removing only a single hydrogen bond at the join between dissimilar monomers reduces τ 500 times (Durkin et al., 1993). Because of the alternating L−D gA sequence (Sarges & Witkop, 1965a), gA dimers can be joined only by an even number of hydrogen bonds. The transition state therefore is likely to be where the dimer is stabilized by four hydrogen bonds.

Table 1: Effects of Membrane Modifiers on Membrane Mechanics[a]

membrane modifier	τ (ms)	C_m (nF/mm^2)	d (nm)	ΔG^0_{def} (kJ/mol)	A (kJ/(mol·nm^2))
none	450 ± 82	3.74 ± 0.10	4.98 ± 0.13	−	120[c]
10 μM TX100	1120 ± 203	3.75 ± 0.13[b]	4.97 ± 0.17	2.3 ± 0.7	117.4 ± 0.8[d]
2.5 mM βOG	2920 ± 480	3.85 ± 0.08	4.84 ± 0.10	4.6 ± 0.6	114.4 ± 0.6[d]
cholesterol	82 ± 12	4.76 ± 0.16	3.92 ± 0.13	−4.2 ± 0.6	205 ± 7

[a] Mean ± sd ($n \geq 5$), sd for τ given with two significant figures only; uncertainties in d, $\Delta G^{\ddagger}_{def}$, and A were estimated using Monte Carlo methods (Alper & Gelb, 1990). [b] Measured at 30 μM TX100. [c] From Durkin et al. (1993). [d] Calculated setting $d^{mod} = d^{cntr}$.

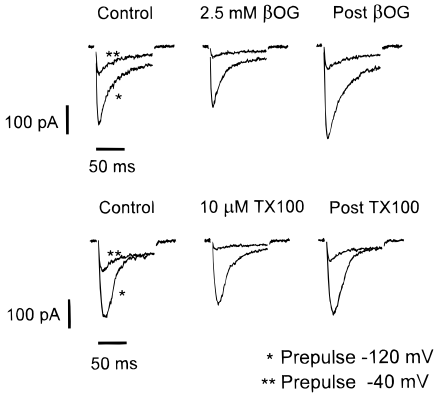

FIGURE 4: Effects of βOG and TX100 on N-type calcium currents. Current traces before, during, and after application of βOG (top) and TX100 (bottom). Inward currents are downward.

function of membrane thickness, N. Mobashery and O. S. Andersen, unpublished observations). To determine A^{mod}, we take μ to be equal to the difference between the equilibrium bilayer thickness (Table 1) and the length of the channel's hydrophobic exterior, 2.17 nm (Elliott et al., 1983) and set $\delta = 0.16$ nm.[2] The resulting values are summarized in Table 1. Addition of βOG or TX100 increases $\Delta G^{\ddagger}_{def}$ by 2−4 kJ/mol with no significant effect on μ, which will be assumed to be unchanged; A^{mod} therefore decreases by 2−5 kJ/(mol·nm^2). Addition of cholesterol decreases ΔG^0_{def} by 4 kJ/mol, and decreases μ by ∼1 nm, which means that A^{mod} increases by ∼80 kJ/(mol·nm^2). One should note, however, that, while ΔG^0_{def} is a directly accessible parameter, the changes in A depend on the somewhat arbitrary choice for the value of δ (cf. eq 8).

Whole-Cell Voltage-Clamp Experiments. The effects of TX100, βOG, and cholesterol on N-type calcium channels were examined using whole-cell patch clamp (Hamill et al., 1981) with Ba^{2+} as the charge carrier. βOG and TX100 reversibly inhibit current flow, and the inhibition varies as a function of the prepulse potential (Figures 4 and 5).

Figure 4 shows the reversible changes in membrane current transients that occur in response to a 1 min application of either 2.5 mM βOG (the top panels) or 10 μM TX100 (the bottom panels). Each panel shows the current transients that were elicited by depolarization of the cell to +10 mV, after a prepulse to either −120 mV, which tends to inhibit inactivation, or −40 mV, which tends to promote inactivation. The peak inward currents are larger after the −120 mV prepulse, which reflects the difference in channel availability at the two holding potentials. The βOG- or TX100-induced current reduction is much larger after the −40 mV prepulse, which suggests that the inhibitory effect of these compounds is related to channel inactivation.

This suggestion is amplified in Figure 5, which shows the average results obtained in experiments where the prepulse

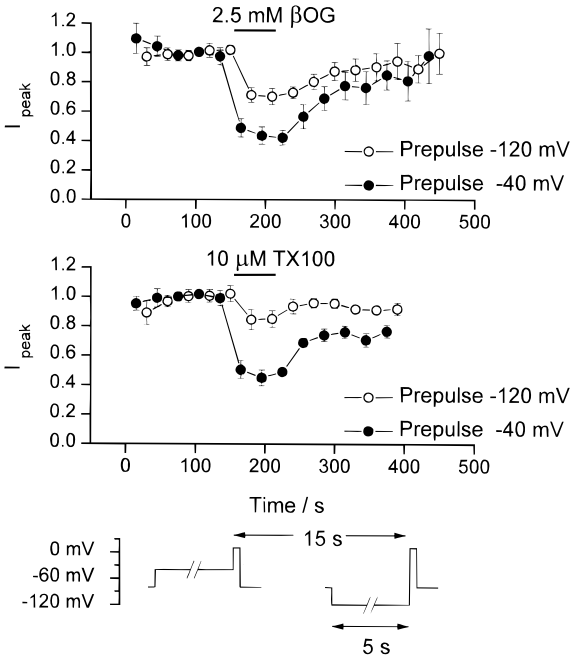

FIGURE 5: Time course of peak current inhibition and recovery after a 1 min superfusion with 2.5 mM βOG (top) or 10 μM TX100 (bottom). The period of superfusion is indicated by the horizontal bars. Each point denotes mean ± sem ($n \geq 3$). The voltage protocol is shown below. Peak currents were measured at depolarizations to +10 mV for 100 ms every 15 s. Each test pulse was preceded by a 5 s conditioning pulse to, alternatingly, either −40 or −120 mV.

alternatingly was either −40 or −120 mV. In the presence of βOG or TX100, the peak currents after a prepulse to −40 mV decreased by 60 or 55%, respectively. The peak currents after a prepulse to −120 mV decreased by only 30 or 15%. After removal of βOG or TX100, the peak currents after the −40 mV prepulse increased to 100 or 80% of control. The peak currents after the −120 mV prepulse increased to 100 or 90% (with prepulses to −140 mV, the cells rapidly became unstable, but there was no current inhibition during exposure to 10 μM TX100 for 1 min). These results show that the reversible current inhibition varies as a function of prepulse potential, which argues that the βOG- or TX100-induced inhibition of the calcium current is due to a shift in the distribution between conducting and inactivated channel states in favor of inactivated state(s).

A possible concern with these experiments is that detergents, at concentrations near their CMC, may cause nonspecific membrane damage and cell lysis (Weltzien, 1979). It is therefore important to note that the effects of βOG and TX100 on calcium channel function cannot be related to such nonspecific membrane damage (or breakdown of the barrier properties). First, βOG and TX100 were used at concentrations that are 10−25-fold below their CMC, which should minimize such deleterious effects. Second, consistent with

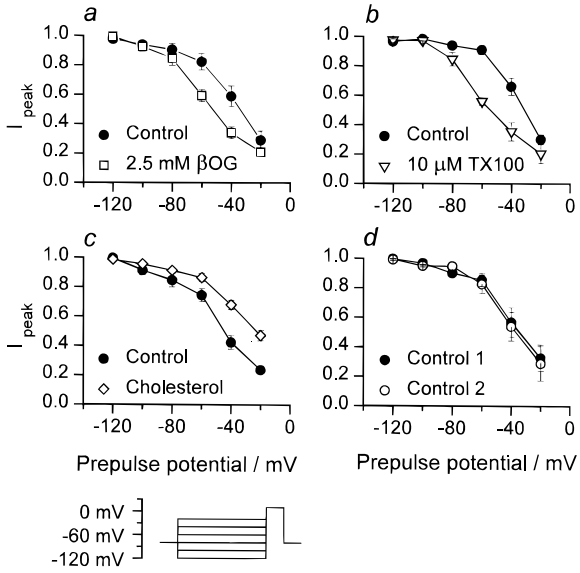

FIGURE 6: Effect of βOG (*a*), TX100 (*b*), and cholesterol (*c*) on calcium channel inactivation. The channel availability was determined from the normalized peak current (at +10 mV) following 5 s conditioning pulses to varying holding potentials. (*d*) In timed controls, the inactivation is unchanged (for each experiment, the second measurement was done ~7 min after the initial control experiment; the second set of control experiments in panel *d* were done after superfusion of the cells with the control extracellular solution). The inset shows the voltage protocol.

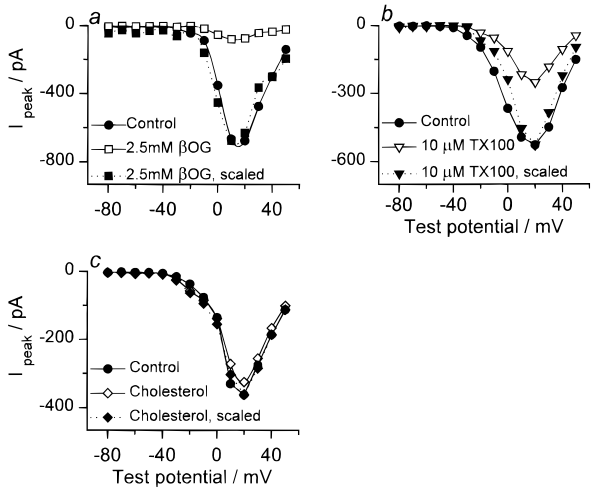

FIGURE 7: Effects of βOG (*a*), TX100 (*b*), and cholesterol (*c*) on the peak current−voltage relation. The stippled curves denote scaled peak current voltage relations in the presence of βOG, TX100, and cholesterol. Each point represents the mean ± sem (n ≥ 3). Current measurements in the presence of βOG and TX100 were done after 2−4 min of superfusion. Measurements with cholesterol-enriched cells were done after 20−24 h of incubation in either control or cholesterol-enriched media.

the use of relatively low βOG or TX100 concentrations, neither compound increased the (non-calcium channel) background conductance, which indicates that there was no membrane damage. Third, the changes in channel function were reversible and varied as a function of prepulse potential (Figures 4 and 5), which shows that the effects of βOG and TX100 are specific, in the sense that the effect of either compound can be altered by alteration of the physiological state of the channels.

The voltage dependence of the effects of βOG, TX100, and cholesterol on calcium channel steady-state inactivation was examined further. The results are shown in Figure 6. βOG (2.5 mM) (Figure 6*a*) and TX100 (10 μM) (Figure 6*b*) produced a 20 mV hyperpolarizing shift of the inactivation curve. The measurements in the presence of βOG and TX100 were done ~7 min after the control measurements. Repeated control measurements, after a similar waiting period, did not change the inactivation curve (Figure 6*d*).

The effect of cholesterol could be examined only after chronic exposure. In cells that had been exposed to a cholesterol-enriched medium for 20−24 h, the midpoint of the inactivation curve was shifted ~20 mV in the *depolarizing* direction, relative to cells exposed to cholesterol-free media for the same period (Figure 6*c*).

In contrast to the shift in the steady state inactivation curves, the channel voltage activation is not affected by βOG, TX100, or cholesterol because the normalized peak current−voltage relations, measured in the presence and absence of amphipaths, are almost superimposable (Figure 7*a*−*c*). As illustrated by the current−voltage relations in Figure 7, there may be a minor, variable current contribution from low-voltage-activated calcium channels. For voltages between −40 and −20 mV, for example, the control current−voltage relation in Figure 7*a* differs from those in Figure 7*b*,*c*. Nevertheless, the dominant current component is due to a single population of N-type calcium channels, as shown by the fact that 5 μM MVIIA ω-conotoxin, which is specific for N-type calcium channels, inhibited 85−95% of the currents (see Materials and Methods). In addition, there is no significant difference between the time course of current inactivation after a 5 s prepulse to −120 or to −40 mV [when fitted with single exponential distributions, the time constants were 26 ± 10 ms (mean ± sd) and 34 ± 11 ms, respectively, $n = 7$], indicating that we examine the current through a homogeneous population of ion channels. Most importantly, neither the 50% decrease in peak current after a 5 s prepulse to −40 mV in the presence of TX100 or βOG nor the 60% increase induced by cholesterol (Figure 6), can be due to low-voltage-activated channels.

The results in Figures 5−7 show that the effects of βOG, TX100, and cholesterol are specific, in the sense that inactivation is altered with no effect on the voltage activation. The effects of βOG, TX100, and cholesterol correlate with their molecular shapes and effects on bilayer stiffness (Table 1). TX100 and βOG, in particular, have quite different chemical structures, which makes it highly unlikely that integral membrane proteins possess specific receptors for these molecules. Moreover, if they did bind, they would interact differently with their binding sites and therefore be expected to have different effects on membrane proteins. The specific and reversible modulation of channel function by TX100 and βOG therefore suggests that bilayer stiffness could be a general determinant of membrane protein function. A more quantitative correlation between the effects of these compounds in planar bilayers and in biological membranes is not warranted, because of the different lipid compositions of these membranes [cf. Sakmann and Boheim (1979)].

Traditionally, modulation of membrane protein function by amphipathic compounds has been ascribed to changes in bilayer "fluidity". But the causal relation between bilayer fluidity and protein function is unclear (Lee, 1991), as also demonstrated by the present results. Detergents would be expected to increase the fluidity of planar lipid bilayers (Lasch et al., 1990), which would increase the rate of

molecular motion and therefore *decrease* the average gA channel duration, as the monomers would tend to move apart more readily. Cholesterol would be expected to decrease fluidity [cf. Yeagle (1985)], which by a similar argument should *increase* channel duration. Maneuvers that alter bilayer stiffness will alter bilayer fluidity as well, but changes in protein function should not be ascribed to the changes in fluidity *per se*.

The changes in gramicidin monomer−dimer equilibrium that are induced by synthetic detergents (Sawyer et al., 1989) or lysophospholipids (Lundbæk & Andersen, 1994) result from changes in the bilayer deformation energy (Table 1). The general ability of amphipathic compounds to alter membrane protein function most likely results from similar changes in bilayer deformation energy, which to a first approximation can be understood by considering the molecular shape of the membrane-active compounds. It is in this respect important to note that the proposal that the membrane deformation energy is an important determinant of membrane protein function is a natural extension of the notion that the spontaneous curvature or bending rigidity is important (Gruner, 1991; Keller et al., 1993). The relationship between molecular shape, bilayer deformation energy, and protein function provides a framework for understanding the control of protein function by the host bilayer.

ACKNOWLEDGMENT

We thank R. E. Koeppe, II, for a gift of gramicidin A, C. Nielsen and L. L. Providence for discussions and experimental assistance, and T. J. J. Blanck, D. Gardner, L. G. Palmer, and S. A. Simon for constructive comments on the manuscript. We also thank the reviewers for their perceptive criticisms.

REFERENCES

Alper, J. S., & Gelb, R. I. (1990) *J. Phys. Chem. 94*, 4747−4751.
Andersen, O. S. (1983) *Biophys. J. 41*, 119−133.
Andersen, O. S., & Koeppe, R. E., II (1992) *Physiol. Rev. 72*, S89−S158.
Andersen, O. S., Sawyer, D. B., & Koeppe, R. E., II (1992) in *Biomembrane Structure and Function* (Gaber, B. P., & Easwaran, K. R. K., Eds.) pp 227−244, Adenine Press, Schenectady, NY.
Andersen, O. S., Lundbæk, J. A., & Girshman, J. (1995) in *Dynamical Phenomena in Living Systems* (Mosekilde, E., & Mouritsen, O. G., Eds.) pp 131−151, Springer-Verlag, Berlin.
Baldwin, P. A., & Hubbell, W. L. (1985) *Biochemistry 24*, 2633−2639.
Benz, R., & Janko, K. (1976) *Biochim. Biophys. Acta 455*, 721−738.
Bolotina, V., Omelyanenko, V., Heyes, B., Ryan, U., & Bregestovski, P. (1989) *Pflügers Arch. 415*, 262−268.
Brown, M. F. (1994) *Chem. Phys. Lipids 73*, 159−180.
Caffrey, M., & Feigenson, G. W. (1981) *Biochemistry 20*, 1949−1961.
Carbone, E., Sher, E., & Clementi, F. (1990) *Pflügers Arch. 416*, 170−179.
Criado, M., Eibl, H., & Barrantes, F. J. (1984) *J. Biol. Chem. 259*, 9188−9198.
Cullis, P. R., & de Kruijff, B. (1979) *Biochim. Biophys. Acta 559*, 399−420.
Dan, N., Berman, A., Pincus, P., & Safran, S. A. (1994) *J. Phys. II 4*, 1713−1725.
Durkin, J. T., Providence, L. L., Koeppe, R. E., II, & Andersen, O. S. (1993) *J. Mol. Biol. 231*, 1102−1121.
Elliott, J. R., Needham, D., Dilger, J. P., & Haydon, D. A. (1983) *Biochim. Biophys. Acta 735*, 95−103.
Evans, E., & Needham, D. (1987) *J. Phys. Chem. 91*, 4219−4228.
Gruner, S. M. (1989) *J. Phys. Chem. 93*, 7562−7570.
Gruner, S. M. (1991) in *Biologically Inspired Physics* (Peliti, L., Ed.) pp 127−135, Plenum Press, New York.
Hamill, O. P., Marty, A., Neher, E., Sakmann, B., & Sigworth, F. J. (1981) *Pflügers Arch. 391*, 85−100.
Hanai, T., Haydon, D. A., & Taylor, J. (1965) *J. Theor. Biol. 9*, 422−423.
Hille, B. (1992) *Ionic Channels of Excitable Membranes*, 2nd ed., Sinauer Associates, Inc., Sunderland, Massachusetts.
Huang, H. W. (1986) *Biophys. J. 50*, 1061−1070.
Hui, S.-W., & Sen, A. (1989) *Proc. Natl. Acad. Sci. U.S.A. 86*, 5825−5829.
Janis, R. A., Silver, P. J., & Triggle, D. J. (1987) *Adv. Drug Res. 16*, 309−591.
Jensen, J. W., & Schutzbach, J. S. (1984) *Biochemistry 23*, 1115−1119.
Johannsson, A., Smith, G. A., & Metcalfe, J. C. (1981) *Biochim. Biophys. Acta 641*, 416−421.
Keller, S. L., Bezrukov, S. M., Gruner, S. M., Tate, M. W., Vodyanoy, I., & Parsegian, V. A. (1993) *Biophys. J. 65*, 23−27.
Konnerth, A., Lux, H. D., & Morad, M. (1987) *J. Physiol. 386*, 603−633.
Lasch, J., Hoffmann, J., Omeleanenko, W. G., Klibanov, A. A., Torchilin, V. P., Binder, H., & Gawrisch, K. (1990) *Biochim. Biophys. Acta 1022*, 171−180.
Lee, A. G. (1991) *Prog. Lipid Res. 30*, 323−348.
Lundbæk, J. A., & Andersen, O. S. (1994) *J. Gen. Physiol. 104*, 645−673.
Maer, A. M., Lundbæk, J. A., Providence, L. L., & Andersen, O. S. (1995) *Biophys. J. 68*, A151 (abstract).
McCallum, C. D., & Epand, R. M. (1995) *Biochemistry 34*, 1815−1824.
Mitchell, D. J., & Ninham, B. W. (1981) *J. Chem. Soc., Faraday Trans. 2 77*, 601−629.
Mouritsen, O. G., & Bloom, M. (1984) *Biophys. J. 46*, 141−153.
Navarro, J., Toivio-Kinnucan, M., & Racker, E. (1984) *Biochemistry 23*, 130−135.
Neher, E., & Eibl, H. (1977) *Biochim. Biophys. Acta 464*, 37−44.
O'Connell, A. M., Koeppe, R. E., II, & Andersen, O. S. (1990) *Science 250*, 1256−1259.
Pope, C. G., Urban, B. W., & Haydon, D. A. (1982) *Biochim. Biophys. Acta 688*, 279−283.
Sakmann, B., & Boheim, G. (1979) *Nature 282*, 336−339.
Salamon, Z., Wang, Y., Brown, M. F., Macleod, H. A., & Tollin, G. (1994) *Biochemistry 33*, 13706−13711.
Sarges, R., & Witkop, B. (1965) *J. Am. Chem. Soc. 87*, 2011−2019.
Sawyer, D. B., Koeppe, R. E., II, & Andersen, O. S. (1989) *Biochemistry 28*, 6571−6583.
Seddon, J. M. (1990) *Biochim. Biophys. Acta 1031*, 1−69.
Unwin, N., Toyoshima, C., & Kubalek, E. (1988) *J. Cell. Biol. 107*, 1123−1138.
Unwin, P. N. T., & Ennis, P. D. (1984) *Nature 307*, 609−613.
Weltzien, H. U. (1979) *Biochim. Biophys. Acta 559*, 259−287.
Yeagle, P. L. (1985) *Biochim. Biophys. Acta 822*, 267−287.

BI952250B